Highly stable forced optoelectronic oscillators and roadmap to integrated clocks

Afshin S. Daryoush
Dept. of ECE, Drexel University, Philadelphia, PA 19104 USA
daryoush@coe.drexel.edu

ABSTRACT

Low phase noise signal generated in a small structure is required for communication and high resolution imaging. Opto-electronic oscillators with their demonstrated low phase noise are popular due to the increasing demand of very clean local oscillator and clock signal sources. Forced techniques of self-injection locking phase locking (SILDPLL) applied on an OEO system reduces the phase noise and suppresses side mode observed in standard OEO with long delays. However, this novel optical feedback technique using self-ILPLL is also employed for phase noise reduction of free-running microwave oscillators. Phase noise reduction of 27 dB at 10 kHz offset has been demonstrated by applying this technique for a 10 GHz state of art DRO, achieving -137 dBc/Hz at 10 kHz offset. A phase noise prediction of this feedback technique is also presented, which very closely corroborates with experimental results. Analysis of SILPLL using the modeling has shown that further phase noise reductions could be achieved, by reducing the residual phase noise of the long delay lines and microwave amplifiers.

In addition, a frequency synthesizer working at K-band is demonstrated using electronically tuned narrowband RF filter in place of fixed narrowband frequency metallic cavity based filters. The synthesizer employs optical transversal filter cascaded with YIG filter to electronically fine and coarse tune the oscillation frequency, as a replacement for fixed frequency high Q metallic filter. Second harmonic generated frequency synthesized signals with close-in to carrier phase noise of -127 dBc/Hz phase noise at 10 kHz are reported by V_π operation of a Mach-Zehnder (MZM) over 18 GHz to 22 GHz with frequency tuning step as small as 20 kHz/pm. A 19'' rack mount system is also constructed and long term stability of 4.5 kHz over 60 min is measured at K-band, while a 3.5 kHz drift is measured for a tabletop realization.

A fully integrated version of this forced OEO is also being pursued to enhance size, power consumption, and cost. A fully monolithic DBR based multi-mode laser is considered with mode-locking method to build frequency stabilized and tunable RF signal generator. The number of the output modes from each laser is adjusted using reflecting bandwidth of distributed Bragg reflector and electro-absorption (EA) modulator for amplitude control, while the phase section in integrated laser system provides frequency tuning. Mode-locking of 60 laser modes results in a highly frequency stable 10 GHz RF beat-notes with a calculated phase noise of -150 dBc/Hz at 10 kHz offset frequency.

KEYWORDS

Dielectric resonator oscillator, self-injection locked and phase locked loop, fiber optic delay line, opto-electronic oscillator, optical feedback, YIG filter, fiber Bragg grating, optical transversal filter, dual drive Mach-Zehnder modulator, distributed Bragg reflector, phase modulator, electro-absorption modulator, multi-mode laser.

1. INTRODUCTION

High frequency microwave oscillators become popular with the increasing need for high speed data transmission. Opto-electronics oscillators [1] used as promising way for creating high frequency RF signal with great purity perfectly meet this demand. Oscillator phase noise reduction can be achieved by forcing free-running oscillator using injection locking (IL) [1] and phase locked loop (PLL) [2]. While IL technique are easy to implement, the phase noise in the close-in offset frequencies is degraded due to frequency detuning and limited locking range as explained in [3]. On the other hand, the high gain loop filter enables the PLL to remove the close-in phase noise significantly, while far away offsets suffers from a higher noise. Sturzbecher *et al*. demonstrated that in externally forced oscillators, a better phase noise characteristics for both close-

Quantum Sensing and Nano Electronics and Photonics XV, edited by Manijeh Razeghi, Gail J. Brown, Jay S. Lewis, Giuseppe Leo, Proc. of SPIE Vol. 10540, 105400X · © 2018 SPIE
CCC code: 0277-786X/18/$18 · doi: 10.1117/12.2297143

in and far-away offset frequencies and a wider locking range are achieved by combining IL and PLL (ILPLL) [4]. However, external reference sources are required in the conventional ILPLL topology, which limits the ultimate phase noise performance.

To bypass limitations imposed by an extremely stable external reference requirement, self-injection locking (SIL) [5] and self-phase locked loop (SPLL) [6] have been proposed. SIL and SPLL are essentially feedback control loops where part of the output signal is delayed and used as reference signal, thus eliminating the need for an external reference. The authors have explained the phase noise reduction mechanism in both optoelectronic oscillator (OEO) and electrical VCO using SIL [7] and SPLL [8] and successfully demonstrated the reduction in both single, dual and triple delay loops. It has been shown in [7]-[8] that long delay is crucial for substantial phase noise reduction, therefore kilometer long optical fiber delay lines have been used to construct the optical feedback since their loss is extremely low compared to electrical delay lines. The loop gain is another key parameter to achieve low phase noise in these feedback systems, as the phase noise reduction is proportional to loop gain [7-10]. The loop gain can be greatly enhanced in SILPLL as opposed to SIL or SPLL alone, thus providing more phase noise reduction. Moreover, combing simultaneously SIL and SPLL, i.e. developing a self-injection locked and phase locked loop (SILPLL) has led to a cleaner spectrum in a wider offset frequency range for a commercially available dielectric resonator oscillator (DRO) at 10GHz [11]. The previously reported results focused on a low cost monolithically integrated distributed feedback (DFB) laser diode with relative intensity noise (RIN) of -120dB/Hz electro-absorption modulators (EAM) [11-13]. However, the lower cost EAM-DFB laser than low cost solution has resulted in a higher optical delay line noise figure, which resulted in a higher amplitude to phase noise (AM-PM) contribution in SILPLL oscillators [13]. Moreover, the use of DFB laser diode with a modular dual drive Mach-Zehnder modulator has resulted in a reduction by 5dB of close-in to carrier phase noise [12].

In the meantime, tunable (C and L-bands) high power (up to 18dBm) fiber lasers with low relative intensity noise (RIN) are available at an acceptable pricing with RIN value of -157dB/Hz [14]. This paper provides comparison of SILPLL DRO at 10GHz using DFB and fiber lasers for fiber lengths of 1km to 7km. Moreover for very long fiber delays, a large number of closely spaced side modes (Δf_L=200kHz.km/L, where L is fiber length in km) are present in the forced oscillator spectra; therefore, multiple feedback paths are introduced to cancel these side modes; performance comparison of SILPLL, SILDPLL, and SILTPLL are made and reported for the first time in terms of side mode level and corresponding timing jitters. Finally, a fully integrated topology using monolithic fabrication has to be explored to reduce size, power consumption, and manufacturing cost.

2. EXPERIMENTS FOR OPTICALLY SILPLL DRO

In this section we will first illustrate the experimental setup of the SILPLL system. Then measured results for DRO employing single loop SIL are presented to explore the length dependency on phase noise reduction. Finally, SILPLL, SILDSPLL, SILTSPLL results are provided to give insights of this novel technique.

The optical delay in SILPLL system is provided by a fiber optic link using Mach-Zehnder modulator (MZM), as shown in Fig., to implement a potential opto-electronically feedback system. A DFB laser diode and Fiber laser performance is compared with same experiment set up. Output of the optical signal is amplified by an EDFA whose output is split into two paths with different delays. Two photodetectors (PD) terminates the optical delay to perform the optical to electrical conversion. In addition, dual drive MZM is implemented here in order to reduce the noise figure of the optical link with the help of push-pull amplifier after DRO. The noise figure with DD-MZM is 32dB while there is 44dB noise figure in single drive configuration.

For the SILPLL operation, the Dual-MZM is driven by the push-pull amplifier after DRO, and the modulated light passes through two different optical delay lines, termed as dual loop SILPLL (SILDSPLL). The SIL signal will divided into two path, one path of the signal is coupled out and directly fed back to the DRO through a circulator, forming the SIL function; another portion is combined with another delay line first and the compared against the non-delayed DRO output to generate a phase error signal for phase and frequency locking, completing the SPLL function. The low frequency phase error is detected by the 'Mixer + LPFA' board that contains a double-balanced mixer as phase detector and an active filter

using op-amp circuit as low pass filter amplifier (LPFA). A 'Mixer+LPFA' board with a low pass cutoff frequency of 100 kHz is used for the SILPLL experiment, and it outputs a DC voltage of 4.6 V when the PLL is in locked state (cf. [8] for more details). An image providing details of the experimental setup of the SILDSPLL system is shown in Fig. 2.

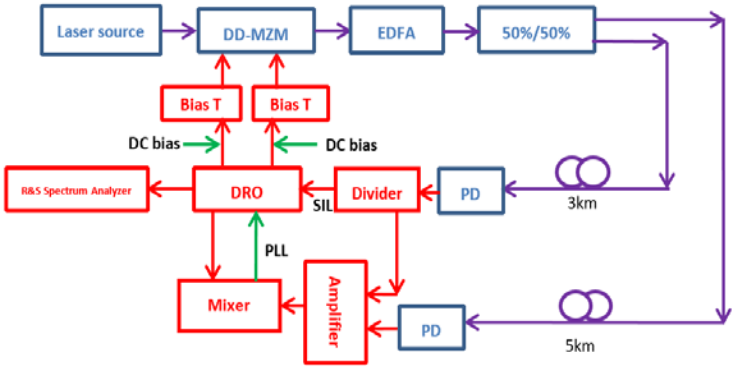

Fig. 1 Block diagram of experimentally demonstrated SILPLL system.

The DRO (DRO100) [14] used as VCO in the experiments has 10dBm output power at 10GHz. The phase noise of this DRO is shown as the black dashed curve in Fig. 3 with -83dBc/Hz at 1 kHz offset and -110 dBc/Hz at 10 kHz offset. The loaded Q of the resonator is found to be about 2000 by curve fitting the measured phase noise to the Leeson's equation [15]. The tuning sensitivity is 280 kHz/V measured at a tuning voltage of 4.6 V. The reason for selecting this particular voltage is that the PLL circuit used in our experiments has a DC output of 4.6 V, when the loop is in locked state.

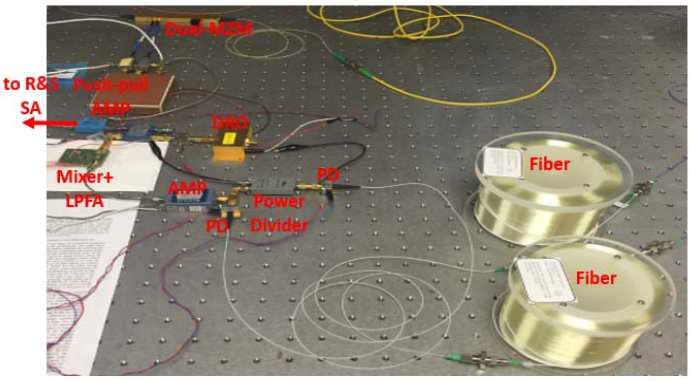

Fig. 2 Image of the SILDSPLL system. DRO represent a dielectric resonator oscillator, PD is the optical photodetector, Dual-MZM is a dual drive Mach-Zehnder modulator, the DD-MZM is driven by low frequency phase locking signal from phase detector and loop filter amplifier (Mixer+LPFA) and push-pull AMP, as a differential amplifier. An R&S phase noise analyzer was used for SSB phase noise measurement.

The SIL experiment can be realized by removing the SPLL path circuits from Fig.. The injection signal level is estimated at about 0 dBm after accounting for cable and connector losses, which results in an injection strength $\rho = \sqrt{P_i/P_O} \approx 0.3$. Half of the 3 dB bandwidth of the oscillator is calculated as $f_{3dB} = f_o/2Q = 2.5$ MHz. Simulation and measured phase noise of SIL using different laser sources are shown in Fig. 3. The newly introduced fiber laser which has lower RIN noise (as low as -157dB/Hz) compare with DFB laser (RIN=-120dB/Hz) [16] is used here to overcome the plateau that appears in that paper starting from 8kHz to 50kHz. From the measured results, single side-band (SSB) phase noise decreases as the RIN decreases; phase noise of -103 dBc/Hz and -131 dBc/Hz are achieved at 1 kHz and 10 kHz offsets respectively in the case of 4km delay line as depicted in Fig. 3. In the SILPLL experiments, the injection locking loop signal strength is kept at $\rho = 0.3$.

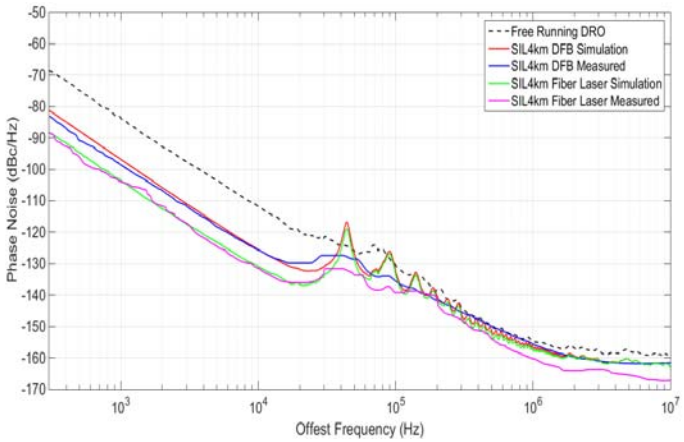

Fig. 3 Comparison of measured and simulated single side band (SSB) phase noise of the free-running (dash line) and forced SIL DRO employing either a DFB laser diode or a fiber laser.

For the SPLL portion, a power level of 10 dBm results in a phase detector sensitivity, K_d, of 0.1 V/rad, and the DRO tuning sensitivity, K_o, of 1758 rad/V. The measured and analytical predicted SSB phase noise performance of SILPLL using different DFB and fiber laser sources are compared in Figures 4-6 for a number phase locking loops. The comparison made here using the DFB and fiber lasers for the same delay lines for injection locking port, but increase the number of the loop for phase locking. Fig. 4 shows the SSB phase noise performance comparison of DFB and fiber laser using single phase locking combine with single injection locking. There appears two different high power spurs peak at 35kHz and 70kHz with power level -83dBc, -93dBc respectively (cf. Table 1). Dual loop implementation of SILDSPLL system is also compared for DFB and fiber laser. It uses the advantage that different delay line will create side mode peak periodically but at different positions. So two aharmonic delay line lengths will interfere with each other, which results in some of the side mode peak suppression. The SSB phase noise performance using dual loop phase locking is depicted in Fig. 5. One side mode peak at 70kHz appears in the spectra for this set up (cf. Table 1).

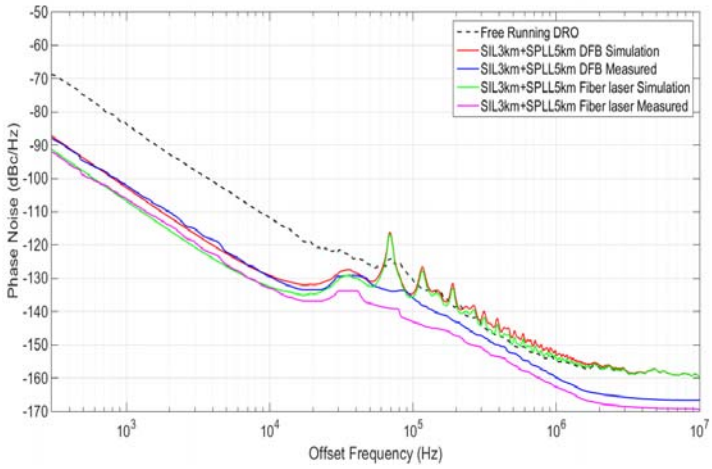

Fig. 4 Comparison of measured and simulated SSB phase noise of the free-running (dash line) and forced SILPLL DRO employing either a DFB laser diode or a fiber laser.

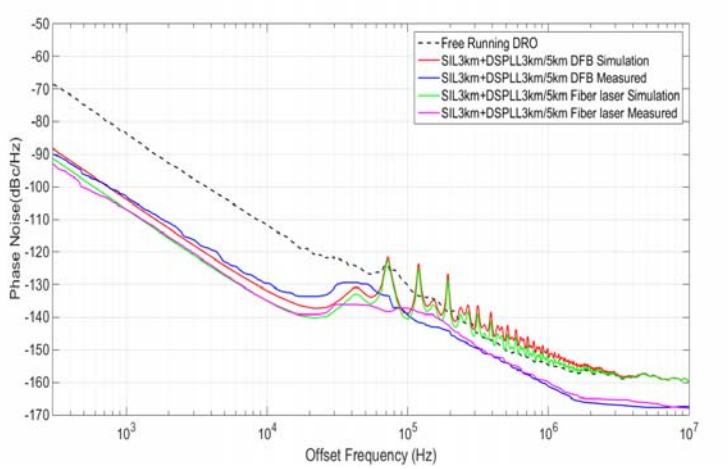

Fig. 5 Comparison of measured and simulated SSB phase noise of the free-running (dash line) and forced SILDPLL DRO employing either a DFB laser diode or a fiber laser.

The successful using dual loop provide us possibility to completely get rid of side mode peak using triple loop for system. The power level of triple need using one more coupler and power level need to be adjusted to keep triple loop provide same level of output. The performance using triple loop phase locking is shown in Fig. 6, which provides a SSB phase noise of-137dBc/Hz at offset frequency 10kHz using the current amplifier of -80$dBrad^2$. A SSB phase noise of -140dBc/Hz at offset frequency 10kHz is also predicted using an amplifier with a flicker frequency -95$dBrad^2$.

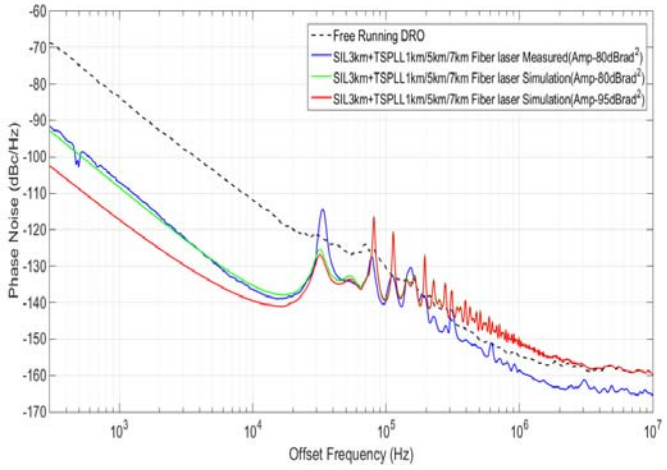

Fig. 6 Comparison of measured and simulated SSB phase noise of the free-running (dash line) and forced SILTPLL DRO employing either a fiber laser and using amplifiers with -80 or -90dBrad^2 residual phase noise.

A number of side modes peaks are expected for a very long fiber delay line lengths and the measured results are depicted in Table 1 for different methods of SILPLL. The results depicted identifies the highest and the closest to carrier peaks; as depicted multiple phase lock loop provides a significant side mode suppression. The side mode rejection has an important impact on the timing jitters of the oscillator, as it is to be used as a clock signal. The overall timing jitters is also calculated based on the integrated noise spectra of the carrier signal from 300Hz to 10MHz. The timing jitter calculation result using the measured SSB phase noise of DFB and fiber laser sources for different configurations are summarized in Table 2. The lowest calculated timing jitters of *6.2fs* is for a fiber laser based SILTSPLL DRO oscillator at 10GHz, while

the highest jitters of *24.2fs* is for a 4km SIL topology using DFB laser. A *2.5fs* timing jitter is expected, when an amplifier is used with flicker frequency of -95dBrad².

TABLE. 1 MEASURED SIDE MODE PEAK POSITION AND VALUES USING DIFFERENT PHASE LOCKING DELAY LOOPS.

SILSPLL	Spurs position	Level	Spurs position	Level
DFB laser	35.23kHz	-83.0dBc	70.53kHz	-94.3dBc
Fiber laser	35.23kHz	-80.5dBc	70.53kHz	-93.2dBc
SILDSPLL	Spurs position		Level	
DFB laser	70.10kHz		-90.2dBc	
Fiber laser	70.10kHz		-91.4dBc	
SILTSPLL	No High Power Spurs			

TABLE. 2 CALCULATED TIMING JITTER PERFORMANCE FOR DIFFERENT FORCED OSCILLATION TECHNIQUES (300HZ-10MHZ)

SIL 4km	Timing Jitter	SPLL 5km	Timing Jitter
DFB Laser	24.2fs	DFB laser	18.1fs
Fiber Laser	15.5fs	Fiber Laser	12.6fs
SIL3km+SPLL 5km		SIL3km+DSPLL 3km/5km	
DFB laser	13.7fs	DFB laser	10.8fs
Fiber laser	9.8fs	Fiber laser	7.0fs
SIL3km+TSPLL 1km/5km/7km	6.2fs	SILTSPLL (using -95dBrad² Amplifier)	2.5fs

3. EXPERIMENTS FOR SILPLL OEO

The self-injection locking phase locking SILDPLL OEO set-up is described in Fig. 7. The low RIN fiber laser (TWL-C-HP-M) is used to provide wavelength tunable laser signal. The signal transmits through optical fiber to create the delay line and then received by photodetector (DSC50S) to set signal pass through narrow band filter. Narrow band filter is the core of the OEO, which is use to select the oscillation frequency. High Q metallic filter is the classic design in use but it needs mechanical adjusting which is not suitable for computer control system based OEO described in Fig. 7. YIG [16] filter will be introduced in this paper to replace the role of high Q metallic filter. Meantime, in order to compensate for poorer frequency selectivity of a widely tunable YIG filter, a narrowband optical transversal filter [17, 18] realized by using chirped fiber Bragg grating (CFBG).

Beside the optical frequency selectivity, self-injection locking [19], self-phase locking [20] and their combination SILPLL [21] is also applied to provide reduction for synthesizer phase noise in both close in and far away to the carrier frequency. The block diagram outside the dotted square depicts SIL and DSPLL [22, 23] simultaneously. There are two paths for modulated signal after MZM, one transmits the main loop of OEO and the other loop is split into two using as 3 km and 8 km dual phase locking signal. The combined phase locking signal is then inputted to a custom design 'Mixer+LPFA' board (block in Fig. 7). A double balanced mixer is integrated on this board with a low pass filter amplifier (realized using Op-Amp circuits) to work as phase detector and low pass portion of the PLL. The phase error of the OEO main loop is compared with the dual delay lines of the phase locking loop and the phase error signal is fed back to the bias port of MZM. Self-Injection locking signal takes the advantage of phase lock loop path and share the same 3km fiber using in SPLL path. The 3 km SIL signal is split from one PLL signal and directly injected into the power combiner. The injected power level is expressed as $\rho=\sqrt{P_i}/P_o$, with P_i, the injected signal power and Po, the OEO power level.

The novelty of this paper is design, implementation, and testing of high frequency resolution 19" rack-mountable K-band frequency synthesizer using SILPLL OEO. The high resolution tuning is due to fine tuning of an optical transversal

filter using a chirped fiber Bragg grating (CFBG) as dispersive component for narrowband filtering. Second harmonic [24] generation is achieved by V_π biasing of the DD-MZM and its portable use system. Performance of this synthesizer is evaluated in terms of its measured close-in to carrier phase noise and its long term frequency stability over 60 minutes.

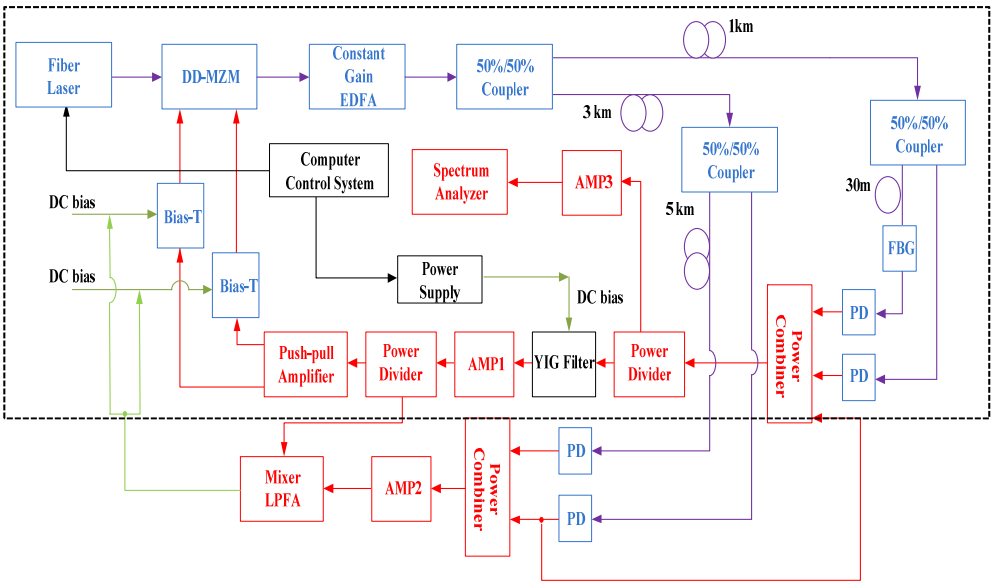

Fig. 7 Block diagram of experimentally demonstrated SILDPLL OEO system.

3.1. Frequency Tuning Techniques and Its Performance

3.1.1. Coarse Tunability Using YIG Filter: YIG filter is attractive in its very broad tuning range and its easily computer control set-up. Using system depicted in Fig. 1, with the tuning of YIG filter, the coarse tuning of synthesizer is achieved as 50 MHz/mA in Fig. 8. The highest resolution for power supply Agilent E3631A working at constant current mode is 1mA. A higher frequency tuning resolution and narrowband filtering is achieved by dispersive CFBG based transversal filter as opposed to fiber based [24].

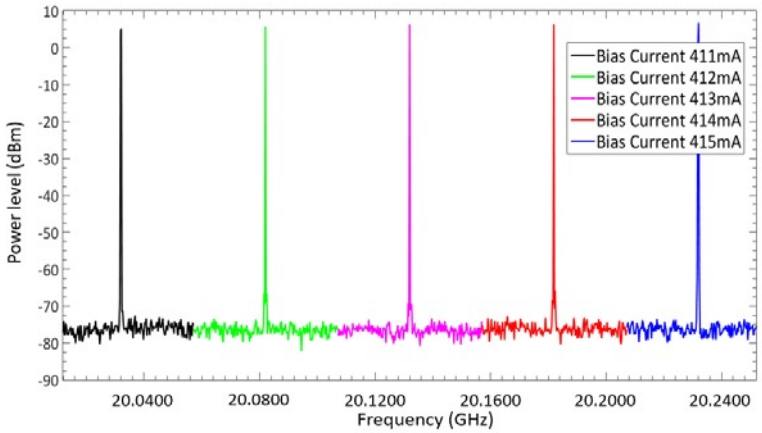

Fig. 8 Synthesizer output frequency versus YIG filter current tuning.

3.1.2. Fine Tunability Using Transversal Filter: An optical transversal filter, as reported in [21] could provide a narrowband filtering of microwave signals. First order transversal filter is depicted in Fig. 9. One optical signal is divided into two paths, one path is using as the reference while another is use to create the delay represent in equation (1).

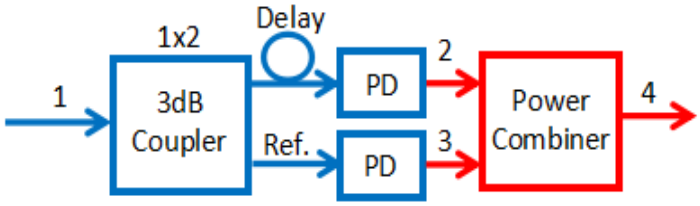

Fig. 9. 1st Order optical transversal filter using 3dB couplers and optical delay.

The filter transfer function in terms of RF frequency is given:

$$H(\omega)=|1+\cos[\omega(\tau_d+\tau_D)]|/2 \quad (1)$$

τ_d is the fiber delay at fiber laser wavelength. It's related to the length difference ΔL between reference and delayed. $n(\lambda_o)$ in equation is refraction index at wavelength λ_o.

$$\tau_d=\Delta L(\lambda o)/c \quad (2)$$

τ_D is the term due to fiber dispersion and expressed as:

$$\tau_D=D\Delta(\Delta\lambda) \quad (3)$$

In equation (3), D is the dispersion parameter in unit of ps/nm/km, while $\Delta\lambda$ is difference between the optical source wavelength and the original wavelength. The tuning performance of transversal optical filter cascaded with a commercially available YIG filter (Tektronix 183-60) is depicted in Fig. 10. Using fiber Bragg grating module (DCM-20A-SCA Motorola) for creating this delay, the dispersion is D = -150 ps/nm and delay τ_d is about 20 ns. This delay creates 40 MHz null to null passing band, which is too wide compared with high Q transversal filter needed; therefore, a 30 m of SMF-28 fiber added to reduce passband filter and achieve a null to null bandwidth to around 4.5MHz. Meanwhile, because of power imbalance introduced by FBG, attenuator and amplifier is required to balance output signal level of two arms. The achieved tuning sensitivity is 20 kHz/pm using pico-meter resolution of the fiber laser (TWL-C-HP-M). The wavelength tuning range for this fiber laser is 40 nm, which results in an overall tuning range can reach up to 400 MHz. This fine tuning can easily cover the tuning gap that exist due to the coarse tuning of 50 MHz/mA achieved by YIG filter.

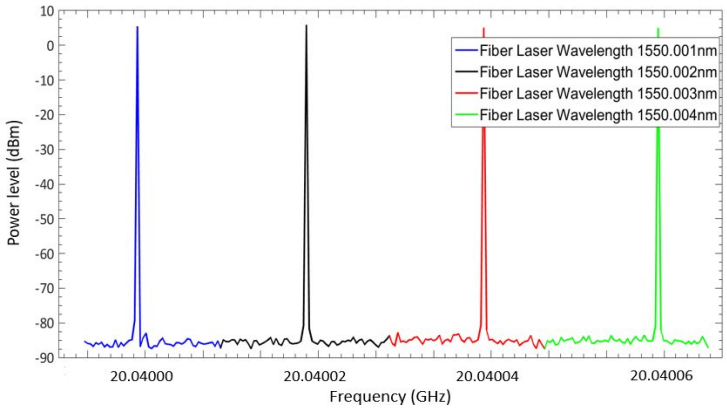

Fig. 10 Synthesizer output frequency versus optical wavelength tuning.

3.2. PHASE NOISE PERFORMANCE AND STABILITY TEST

3.2.1. Phase Noise Performance of K-band Synthesizer: The phase noise performance is important to show the cleanness of this OEO based system. With the helping of forced techniques SILDSPLL, both close in to the carrier and far to the carrier phase noise experience reduction. The phase noise is -99 dBc/Hz at offset frequency 1kHz and -127 dBc/Hz at offset frequency 10 kHz in Fig. 11. The side mode peak is also successfully suppressed using narrow band filter and phase locking system for this OEO.

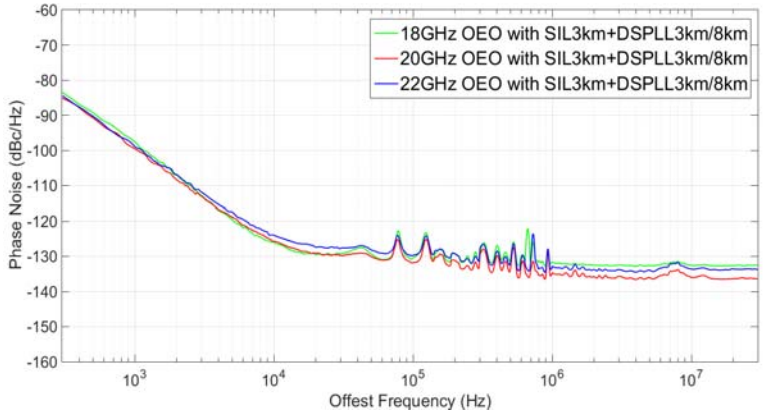

Fig. 11 K-band synthesizer phase noise performance at different frequency.

3.2.2. Long Term Stability of K-band Synthesizer: Long term stability is also reported here. The YIG filter is a temperature and current sensitivity component. Its performance will be affected by the current shift and temperature variation. Because of the fact that phase locking signal is not strong enough to stabilize the YIG filter, any current deviation in the constant current source will inevitably change the center frequency of synthesizer output. The long term stability is depicted in Fig. 12. The 30 min max hold will result in 2 kHz drift in the center frequency shift, while 60 min max hold results in 3.5 kHz drift. The long term stability is estimated to be under +/-0.1 PPM.

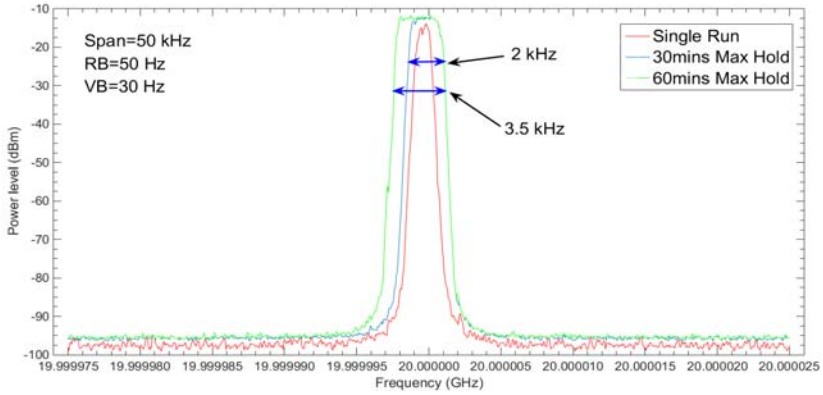

Fig. 12 Long term frequency stability at 20 GHz of a table top K-band synthesizer.

3.3. 19'' SYSTEM REALIZATION FOR PORTABLE USE

The overall system is implemented into 19'' rack mount system for portable use after successfully realized experiment table. Fig. 13a and Fig. 13b depict the top view and front view of the system respectively. The measured phase noise of the OEO system is depicted in Fig. 14. The measured phase noise level is -98 dBc/Hz at offset 1 kHz and -127 dBc/Hz at offset frequency 10 kHz. The performance is similar to the one reported in section 3.2. The stability condition is also tested using same time gap period. 30 min stability testing will bring 3kHz center frequency shift while 60 min time period will cause 4.5kHz synthesized frequency shift. The performance is depicted on Fig. 15.

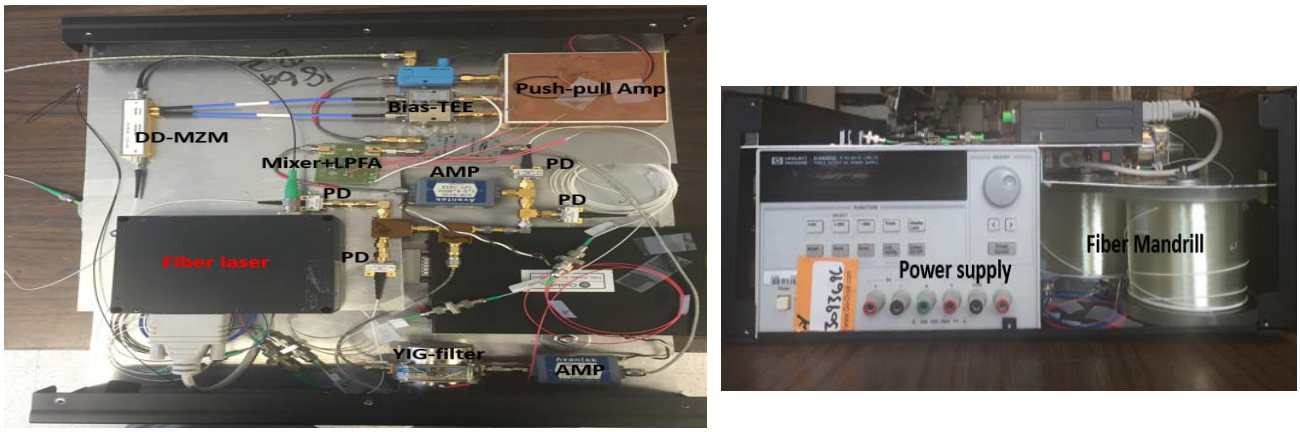

(a) (b)

Fig. 13 Images of the K-band synthesizer OEO system, a) top, b) front views.

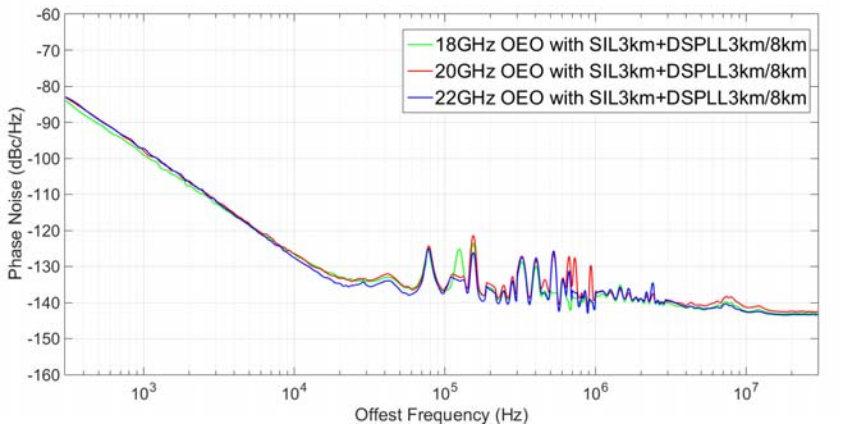

Fig. 14 Measured phase noise of K-band OEO in a 19" rack-mountable box.

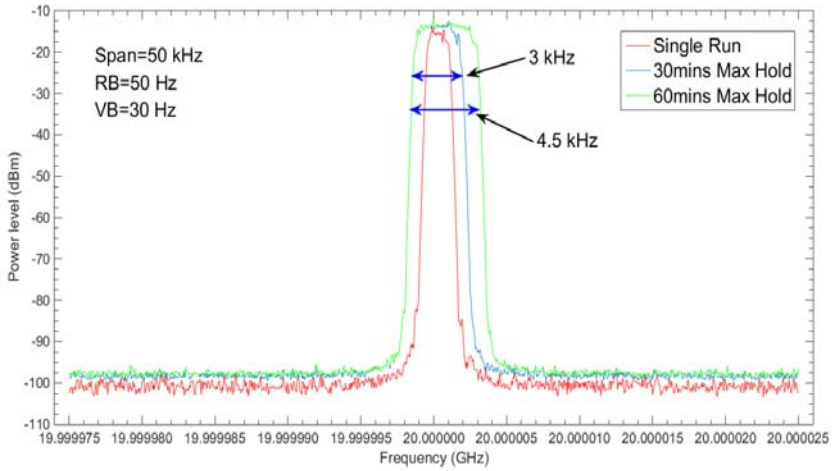

Fig. 15 Long term frequency stability at 20GHz of a 19' rack-mountable box.

4. MONOLITHICALLY INTEGRATED OEO

A fully integrated topology using monolithic fabrication that are compatible with Si-Photonics are to be explored to reduce size and cost while temperature sensitivity is also to be improved. Chip level multi-mode laser generates beat-note at radio frequencies [25], but those suffer from a very poor phase noise characteristics. To properly address this poor close-in to carrier phase noise, forced oscillations are combined with monolithically integrated devices in this paper. The block diagram showed in Fig. 16 provide the laser configuration. The laser consists of 4 major sections [26] including distributed Bragg reflector (DBR), gain medium, phase tuning section and electro-absorption modulator. Distributed Bragg reflector is used as a filter to select laser output frequency [27]. When increasing reflection band, DBR based multi-mode laser will provide more number of modes with appropriate frequency separation decided by cavity length. Two lasers pairs will share one DBR (DBR section) using a Y-junction in our simulation design.

Meanwhile, in order to minimize the effects introduced by shared DBR, the length of DBR is increased. Phase tuning section [28] in the laser set up works for the frequency tuning. It works as the phase modulator in the DBR laser. Different DC bias voltages will be applied to drive different output frequency from each multi-mode laser [29]. The output Y-junction provides input to a high speed photodetector for efficient detection of the ultra-stable beat-notes RF signal. Gain medium part is designed using InGaAsP-InAsP multi quantum well structure for operation at about 1550 nm, where a threshold current of about 30 mA is estimated. Finally, the electro-absorption modulator is integrated in the simulation set-up, where effective absorption coefficient is changed per both wavelength and biasing voltage [30]. The electro-absorption amplitude modulator is applied to effectively control the number of output laser modes using its different absorption rate. The novelty of this paper is modeling of two multi-mode lasers that share a DBR section for the first time. Moreover, the simulation explores phase and amplitude modulations to adjust the beat-note frequency and the number of laser modes. An ultra-stable RF signal is expected using this novel generation.

The challenge is to convert these designs to monolithically integrated components using designs that matches with any of heterogeneously integrated Si-Photonics foundries. Likely, a number of viable options are now available to implement fully integrated active and passive devices. European organization have made significant investments in development of generic photonic foundry platform infrastructures for InP-based heterogeneous Si-Photonics.

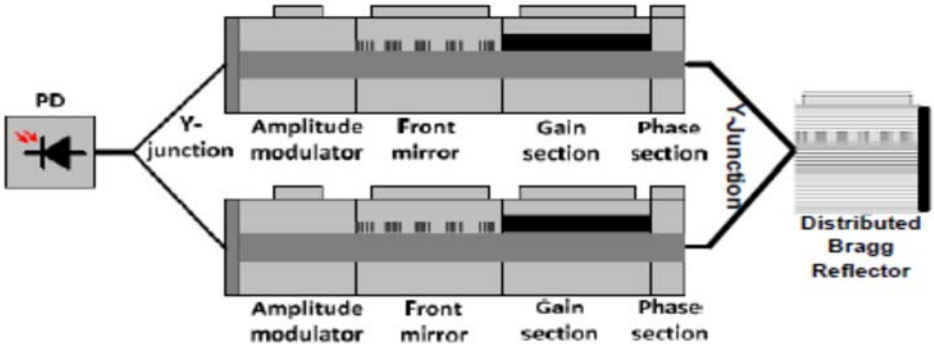

Fig. 16. Block diagram of RF beat-notes generation laser system using DBR based multi-modes laser pairs, where integrated lasers are based on [26].

4.1. Performance Of Multi-Mode DBR Laser Using Different DBR Bandwidth

Distributed Bragg reflector is the core part for selecting laser oscillation frequency. The DBR bandwidth relies on the reflective index of different layer while the frequency separation is decided by laser cavity length. The bandwidth of DBR is first designed as 200 GHz in OptiGrating tool (from Optiwave Inc.). The optimized design parameters are applied to system level design software Lumerical Interconnect (from Lumerical Solution, Inc.) for Fig. 1 block diagram realization. Fig. 17 show the simulation results under different mode gaps. In Fig. 17a, the mode gap is setting up for 250 GHz, so

other mode is outside the passing band of DBR. In this way, we will have 1 modes existing in passing band for both lasers (they overlap each other). Then, other two designs for frequency gap equals to 40 GHz and 15 GHz are depicted in Fig. 17b and Fig. 17c. The DBR passband is still set at 200 GHz, where 5 modes and 13 modes separately for these two conditions. In the theory using beat-notes generating RF signal, the more number of available modes will bring result in a more stable beat-notes. A very broad passband for DBR is then a very promising way to realize this goal. In fact, 60 modes for each laser is depicted in Fig. 17d by selecting a DBR bandwidth of 900 GHz with a frequency separation of 15 GHz.

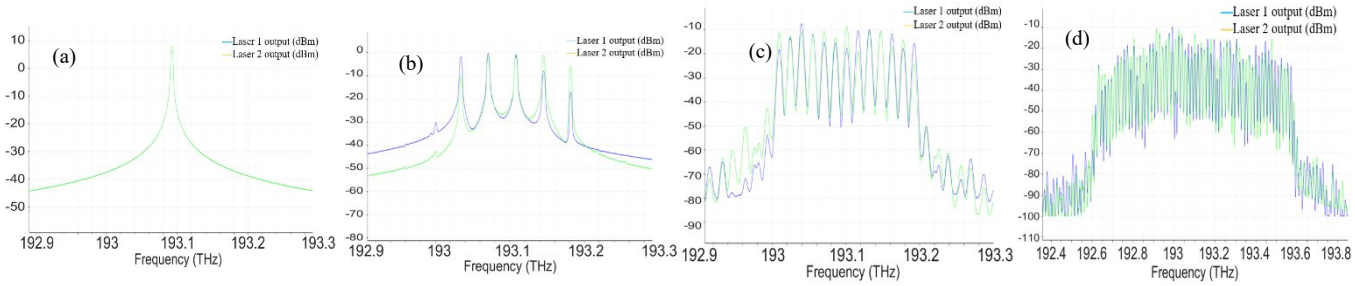

Fig. 17. Performance of multi-mode laser output using different DBR frequency separation; a) single-mode, b) 5 modes, c) 13 modes, and d) 60 modes.

4.2. Phase and Amplitude Modulation Applied in The DBR Based Laser Design

With this 60 modes using an optimized DBR section design, performance of a DBR laser is simulated by employing both phase tuning section and electro-absorption modulator based amplitude control. Improved beat-note RF signal based on this modes number is discussed in this section.

4.2.1. Phase tuning method and results: Output frequency tuning for each DBR laser pairs is realized using phase modulation section. By applying different DC biasing voltage, the multi-mode laser output will shift at the same time by employing a similar design structure as (cf. section II), but for various applied DC voltage. Frequency tuning of a single mode laser is depicted in Fig. 18a with a 70 GHz optical frequency tuning and 70GHz RF beat signal from photodetector. For the case of 5 modes laser pairs (cf. Fig. 18b), 10 GHz RF frequency beats are generated, while 5 GHz RF frequency beats are generated for 13 modes and 60 modes lasers, as respectively depicted in Fig. 18c and d. Simulation results of Fig. 18 depict the potential generation of stable RF signal ranging from 5 GHz to 70 GHz using multi-mode lasers. With adjusting the DC bias voltage control of phase modulator, frequency synthesis could be made from 5-70GHz.

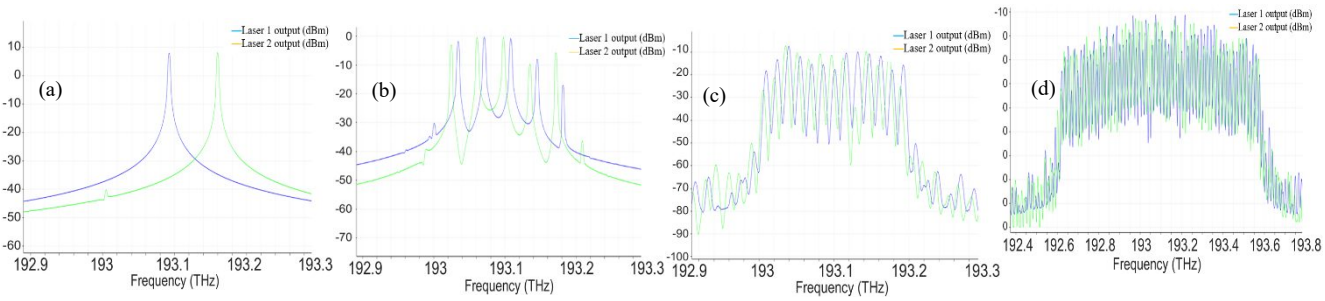

Fig. 18. Performance of multi-mode laser output using phase tuning for different DBR bandwidth and selected frequency beats; a) single-mode, b) 5 modes, c) 13 modes, and d) 60 modes.

4.2.2. Mode number control using EA modulator: Mode number adjustment is another useful function for multi-mode laser based beat-notes generation. Integrated EA modulator (EAM) is applied here using its different effective absorption coefficient value at different wavelength using applied voltage. The used simulation absorption coefficient is from [30] and the designed EAM length is selected to be about 20 um. Using equation (4), the calculated wavelength dependent loss is applied to the multi-mode laser.

$$I = I_0 e^{-\alpha x} \tag{4}$$

The simulated result is based on 60 modes multi-mode laser output. Simulation result is shown in Fig. 19 using -0.5V biasing voltage for this integrated electro-absorption modulator. Because the EAM introduces a higher attenuation at high frequency region, the number of available modes of multi-mode laser at higher frequencies are reduced further, hence effectively adjusting mode numbers in multi-mode laser. Furthermore, with higher reverse biasing voltage of electro-absorption modulator, a higher attenuation at higher frequency region that results in further reduction of the modes that contribute to the beat-notes RF signal (cf. Fig. 20). The resultant RF signal is then studied in terms of close-in to carrier phase noise.

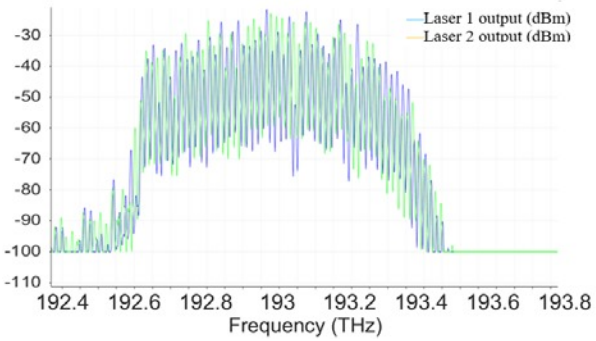

Fig. 19. Frequency distribution control of 60 multi-mode power levels of two lasers with EAM bias voltage at -0.5V.

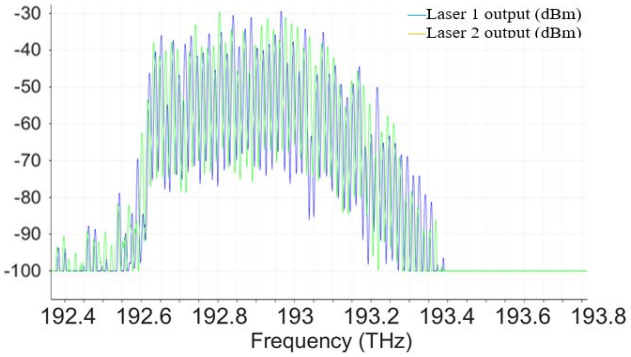

Fig. 20. Control of 60 multi-mode laser output with EAM bias voltage at -1.5 v.

4.2.3. Mode Locked Beat-Notes Performance Under Different Modes Number: In order to compare RF signal charcateristics using different number of modes, the frequency difference for multi-mode laser pair is set to fixed 10 GHz. The close-in to carrier phase noise at 10GHz is then compared for different mode number cases. Meantime, mode locking [31] technique is applied on the multi-mode laser output for simulation comparison with free running result. The best 10 GHz beat-notes simulation result is for 60 modes, as depicted in Fig. 21, with frequency resolution of 50 Hz over 200 kHz frequency span. In order to check stability of close in to carrier frequency, small span value as low as 2 kHz is also displayed in Fig. 22. There is no significant side mode peak appearing in the simulation, so the beat-notes RF output is stable and clean.

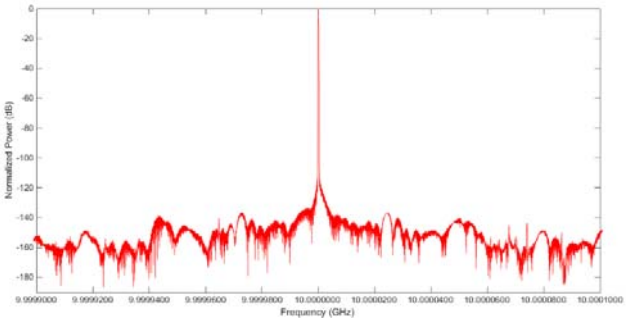

Fig. 21. Simulated frequency spectra of 10GHz beat signal for mode-locked 60 modes (frequency resolution of 50 Hz and span of 200 kHz).

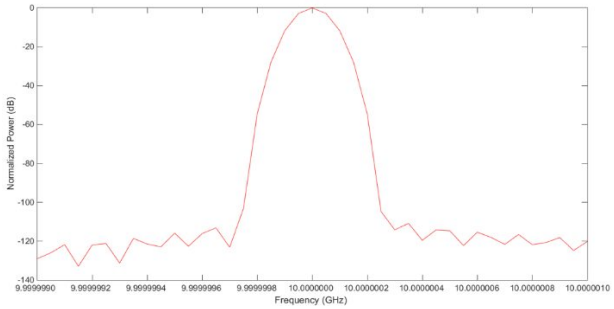

Fig. 22. Simulated frequency spectra of 10GHz beat signal for mode-locked 60 modes (frequency resolution of 50 Hz and span of 2 kHz).

Other simulation result using different modes number and the case without mode locking is also provided in Table 3 in terms of close-in to carrier phase noise at 10GHz. Mode locking technique demonstrated reduced phase noise compared with free running laser beat-notes RF signal. The best performance is -150 dBc/Hz at offset frequency 10 kHz in mode lock condition in comparison to -120 dBc/Hz for free running beat-notes. In addition, at samll mode number value, the simualted result sometimes shows lower phase noise value when compared with large mode number phase noise performance (e.g., phase noise at offset frequncy of 1 kHz is worse for mode numbers of 13 than 5 modes), especially at free running case. That is because when the number of the mode is comparatively small, the beat-notes doesn't show any advantages using modest increase in mode numbers. The small difference is simply exasperated by random oscillation of each mode generated in multi-mode lasers. However, when the mode number reaches above 50, random oscillation is forced to be coherently locked to other modes, hence having a greater RF signal stability.

TABLE 3 SIMULATED PHASE NOISE FOR 10GHZ RF BEAT NOTES USING DIFFERENT MODE NUMBER UNDER WITH OR WITHOUT MODE LOCKING

Mode Number	Free Running @1KHz	Mode locking @1KHz	Free Running @10KHz	Mode locking @10KHz
1	-100 dBc/Hz	-78 dBc/Hz	-120 dBc/Hz	-105 dBc/Hz
5	-98 dBc/Hz	-120 dBc/Hz	-120 dBc/Hz	-120 dBc/Hz
13	-90 dBc/Hz	-117 dBc/Hz	-118 dBc/Hz	-130 dBc/Hz
20	-98 dBc/Hz	-120 dBc/Hz	-120 dBc/Hz	-140 dBc/Hz
60	-105 dBc/Hz	-130 dBc/Hz	-120 dBc/Hz	-150 dBc/Hz

5. CONCLUSIONS

Optical feedback technique is an effective method for oscillator phase noise reduction. Phase noise of -137 dBc/Hz at 10 kHz offset is measured for a 10 GHz DRO employing SILTSPLL with 1 km, 5km and 7km delays. Analytical simulation for phase noise of DRO with feedback loops is employed to compare to the measurement results, which are in great agreement with the experimental results. Our analysis using the proven modeling has justified that the current limitation of the system performance is due to RIN of laser source and flicker frequency of low noise amplifier using in phase locking loop. By reducing the optical source RIN level to the reported level of -170 dB/Hz and decreasing flicker frequency to the state of art as low as $-130dBrad^2$, phase noise of -148 dBc/Hz is predicted at 10 kHz offset for this 10 GHz DRO.

In addition, this paper also reports on realization of a SILPLL OEO frequency synthesizer over K-band. Phase noise reach -127 dBc/Hz at offset frequency 10 kHz over 18-22 GHz with the smallest tuning step of 20 kHz/pm achieved as the fiber laser wavelength is tuned in a highly dispersive CFBG of the optical transversal filter, as opposed 33kHz/nm for SMF-28 [24]. A frequency drift of only 3.5 kHz is measured over 60 min resulting under +/-0.1 ppm frequency stability.

This paper also demonstrates design of a monolithically integrated OEO, where a fully chip level integrated DBR based multi-mode laser is used to achieve as highly stable RF source. Two multi-mode lasers with phase tuning section and amplitude modulation are integrated together to control the output frequency and the number of laser modes contributed to the RF beat-note from Photodiode output. The beat-notes output simulation results show tuning range starting from 5-70 GHz, while the effective mode numbers are adjusted from 1- 60 modes. The frequency stability of RF beat-notes signal is also calculated with the most promising phase noise result of -150 dBc/Hz at 10 kHz offset for 10 GHz beat-note RF output under mode lock techniques with maximum simulated modes number of 60.

ACKNOWLEDGMENTS

This work presented on SILPLL DRO and K-band frequency synthesizer is supported under financial support of Synergy Microwave Corp., Paterson, NJ. I would like to acknowledge continuous support and technical collaborations of Prof. Ulrich L. Rohde and Dr. Ajay Poddar. The technical work presented in this invited paper could not be performed without contribution and dedication of my current and past PhD students, Mr. Tianchi Sun and Dr. Li Zhang.

REFERENCES

[1] H. P. Moyer and A. S. Daryoush, "A unified analytical model and experimental validations of injection-locking processes," *IEEE Trans. Microwave Theory Tech.*, vol. 48, no. 4, pp. 493-499, Apr. 2000.

[2] C. McNeilage *et al*., "Review of feedback and feedforward noise reduction techniques," in *Proc. IEEE Int. Freq. Control Symp*., Pasadena, CA, May 1998, pp. 146 – 155.

[3] X.S. Zhou, X. Zhang, A.S. Daryoush, "A new approach for a phase controlled self-oscillating mixer," *IEEE Trans. Microwave Theory Tech.*, vol. 45, no. 2, pp. 196-204, Feb. 1997

[4] D. Surzbecher *et al*., "Optically controlled oscillators for millimeter-wave phased-array antennas," *IEEE Trans. Microwave. Theory Tech.*, vol. 41, no. 6/7, pp. 998-1004, Jun/Jul 1993.

[5] H. C. Chang, "Phase noise in self-injcetion locked oscillators – Theory and Experiment," *IEEE Trans. MTT*, vol. 51, no. 9, pp. 1994 – 1999, Sep. 2003.

[6] G. Pillet *et al*., "Dual-frequency laser at 1.5μm for optical distribution and generation of high-purity microwave signals," *J. of Lightwave. Technol.*, vol. 26, no. 15, pp. 2764-2773, Aug. 2008.

[7] L. Zhang *et al*., "Analytical and experimental evaluation of SSB phase noise reduction in self-injection locked oscillators using optical delay loops," *IEEE Photonics J.*, vol. 5, no. 6, Dec. 2013.

[8] L. Zhang *et al*., "Comparison of optical self-phase locked loop techniques for frequency stabilization of oscillators," *IEEE Photonics J.*, vol. 6, no. 5, Oct. 2014.

[9] A. Poddar *et al*., "Self Injection Locked Phase Locked Loop Optoelectronic Oscillator," *US Patent app*., No. 61/746919, 2012

[10] A. Poddar *et al*., "Integrated production of self-injection locked self-phase loop locked Opto-electronic Oscillators", *US Patent app*. 13/760767, 2013.
[11] L. Zhang *et al*., "Self-ILPLL using optical feedback for phase noise reduction in microwave Oscillators," *IEEE Photonics Technology Letters*., vol. 27, no. 6, pp. 624–627, Mar. 2015.
[12] T. Sun *et al.,* "Oscillator phase noise reduction using optical feedback with dual drive Mach-Zehnder modulator." in *Proc. IEEE Microwave Symposium (IMS)*, Phoenix, AZ, USA, May. 25-29, 2015.
[13] T. Sun *et al.,* "Integrated Implementation of Ultra Stable VCO using Optical Self-ILPLL Techniques." in *Proc. IEEE Microwave Symposium (IMS)*, San Francisco, CA, USA, May. 23-27, 2016.
[14] Online. Available: https://www.oequest.com/cat/1855
[15] Rohde, Ulrich L. *Microwave and Wireless Synthesizers: Theory and Design*. John Wiley & Sons, 1997.
[16] M. Aigle, G. Hechtfischer, W. Hohenester, R. Jünemann, and C. Evers, "A systematic way to YIG-filter-design," in 37th European Microwave Conference, Munich, 2007.
[17] Y. Jiang et al., "A selectable multiband bandpass microwave photonic filter," IEEE Photonics Journal, vol. 5, no. 3, p. 3, June 2013.
[18] J. Mora et al., "Photonic microwave tunable single-bandpass filter based on a Mach-Zehnder interferometer," J. Lightwave Tech., vol. 24, no. 7, July 2006.
[19] L. Zhang et al., "Analytical and experimental evaluation of SSB phase noise reduction in self-injection locked oscillators using optical delay loops," IEEE Photonics J., vol. 5, no. 6, Dec. 2013.
[20] L. Zhang et al., "Comparison of optical self-phase locked loop techniques for frequency stabilization of oscillators," IEEE Photonics J., vol. 6, no. 5, Oct. 2014.
[21] Zhang Li, Ajay K. Poddar, Ulrich L. Rohde, and Afshin S. Daryoush. "Self-ILPLL Using Optical Feedback for Phase Noise Reduction in Microwave Oscillators." Photonics Technology Letters, IEEE 27, no. 6 (2015): 624-627.
[22] A. Poddar, A. Daryoush, and U. Rohde, "Self-injection locked phase locked loop optoelectronic oscillator," US Patent US9088369B2, 2012.
[23] A. Poddar, A. Daryoush, and U. Rohde, "Integrated production of self-injection locked self-phase locked opto-electronic oscillators," US Patent US9094133B2, 2013.
[24] T. Sun et al., "Forced SILPLL Oscillation of X- and K-Band Frequency Synthesized Opto-electronic Oscillators," 2016 IEEE Microwave Photonics (MWP), Long Beach, USA, 2016.
[25] J.D. Bower, "Chip-scale Optical Resonator Enabled Synthesizer," International Frequency Control Symposium, New Orleans, LA, May 2016.
[26] L. A. Johansson, Y. A. Akulova, G. A. Fish and L. A. Coldren, "Sampled-grating DBR laser integrated with SOA and tandem electroabsorption modulator for chirp-control," in *Electronics Letters*, vol. 40, no. 1, pp. 70-71, 8 Jan. 2004.
[27] S. Joshi, C. Calò, N. Chimot, M. Radziunas, R. Arkhipov, S. Barbet, A. Accard, A. Ramdane, and F. Lelarge, "Quantum dash based single section mode locked lasers for photonic integrated circuits," Opt. Express 22, 11254-11266 (2014).
[28] J. S. Barton, E. J. Skogen, M. L. Masanovic, S. P. Denbaars and L. A. Coldren, "A widely tunable high-speed transmitter using an integrated SGDBR laser-semiconductor optical amplifier and Mach-Zehnder modulator," in *IEEE Journal of Selected Topics in Quantum Electronics*, vol. 9, no. 5, pp. 1113-1117, Sept.-Oct. 2003.
[29] L. Hou, R. Dylewicz, M. Haji, P. Stolarz, B. Qiu and A. C. Bryce, "Monolithic 40-GHz Passively Mode-Locked AlGaInAs–InP 1.55-um MQW Laser With Surface-Etched Distributed Bragg Reflector," in *IEEE Photonics Technology Letters*, vol. 22, no. 20, pp. 1503-1505, Oct.15, 2010.
[30] Y. H. Kuo *et al*., "Quantum-Confined Stark Effect in Ge/SiGe Quantum Wells on Si for Optical Modulators," in *IEEE Journal of Selected Topics in Quantum Electronics*, vol. 12, no. 6, pp. 1503-1513, Nov.-dec. 2006.
[31] C. Gordón, R. Guzmán, V. Corral, M. Chieh Lo and G. Carpintero, "On-Chip Multiple Colliding Pulse Mode-Locked Semiconductor Laser," in *Journal of Lightwave Technology*, vol. 34, no. 20, pp. 4722-4728, Oct.15, 15 2016.